

Experimental determination of potential distribution on a CFRP laminate and thermal images of DC and impulse currents: evaluation of connections

J. Montanyà, D. Romero, R. López and G. Tobella

Abstract— Carbon Fiber Reinforced Plastic (CFRP) components are commonly present in new generation of wind turbine blades and aircraft. CFRP components are preferred for its good mechanical strength and low weight. However, CFRP is more vulnerable to lightning currents and arcs. In addition, CFRP can present very anisotropic electric properties that can difficult its lightning protection. In this paper we present two types of tests intended for improving the understanding of electrical properties of CFRP useful for lightning protection. The experimental and simulation study of the potential distribution along a CFRP coupon suggest how the currents are distributed and some defects in the electrical connections. A new method in order to investigate connection effectiveness in full scale wind turbine blades is proposed. The method is minimal invasive. The second part of the paper discusses the possible current paths in different arrangements of connections by means of thermal imaging.

Keywords— aircraft, blades, carbon reinforced plastics, lightning, wind turbines.

I. INTRODUCTION

WIND turbines can be regarded as tall structures where a large portion is under movement and with extensive use of composite materials. Modern turbines can reach altitudes of about to 200 m if we take into account blade lengths of more than 70 m over nacelles at heights of more than 130 m. Large part of the structure corresponds to the

This part should contain the authors' current affiliations, including current address and e-mail.

J. Montanyà Puig is with the Department of Electrical Engineering, Technical University of Catalonia. Barcelona Tech, Terrassa (Barcelona) 08222, Spain (montanya@ee.upc.edu).

D. Romero Duran is with the Department of Electrical Engineering, Technical University of Catalonia. Barcelona Tech, Terrassa (Barcelona) 08222, Spain (romero@ee.upc.edu).

R. López Scutaró is a visiting undergraduate student with the Department of Electrical Engineering, Technical University of Catalonia. Barcelona Tech, Terrassa (Barcelona) 08222, Spain (ricardo.lop89@gmail.com).

G. Tobella is with the LABELLEC high voltage laboratory, Terrassa (Barcelona) 08223, Spain, labellec@ingesco.com

rotor blades which is in motion. Typically, multi-megawatt wind turbines can present rotating speeds up to 20 turns per minute. At these rotating speeds, blade tips can reach velocities of several tens of meters per second. This effect may play some important role on the lightning leaders initiation [1]. In addition, rotor blades are built with composite materials such as glass fiber and carbon fiber reinforced plastics (CFRP) [2]. All these factors contribute to increase the complexity of the lightning protection of blades and promoted the efforts of international working groups (e.g. [3]).

Lightning protection of wind turbines is currently covered by the IEC 61400-24 standard [4]. Different tests for blades are described in its annex D. Those tests are intended to verify the Lightning Protection System (LPS) performance of blades. High voltage tests are intended to verify the lightning attachment efficiency of air terminals. Once lightning channels are attached to a blade, the conduction of the current is verified in the laboratory with high current impulse tests. High current tests are very useful to verify down conductors, connection components and investigate damage mechanisms in blades. During the design of a new blade employing CFRP components, one of the main challenges is to verify the electrical connections of the LPS to the CFRP elements (e.g. spar). The anisotropic electric properties of CFRP and the difficulties of implementing connections with minimal CFRP erosion make the connection to CFRP a non-trivial task.

Electrical properties of CFRP used in wind turbines are not extensively available in literature (e.g. [5-8]). Most of the publications dealing with CFRP properties comes from aerospace research (e.g. [6]). A review of the methods used for extracting conductivities in the anisotropic CFRPS can be found in [6]. A recent application of characterization of a CFRP is found in [7]. In [7] the authors calculate the resistances of an array of electrodes in a CFRP coupon. The authors used sub-ampere DC and impulse currents. An interesting result is the surface potential distributions along the measured electrodes.

Inspired in [7] in this paper we obtain the surface potential

Preprint of the:
Asia-Pacific International Conference on Lightning (APL),
2015
Nagoya, Japan

distributions on a CFRP coupon. In addition to consider only the electrodes face we also inspected the potentials of the opposite face. Then the potential differences between symmetrical points of both sides are computed. The method and results suggested a new method useful in order to verify the effectiveness of CFRP connections of the lightning protection system (LPS) on wind turbine spars. In the next section thermal images of the CFRP coupon submitted to DC and impulse currents are presented and discussed. The experiments are intended to investigate the current path in different electrode configurations.

II. INVESTIGATION OF POTENTIAL DISTRIBUTION ON A CFRP COUPON

A. Description of the experiment

Two electrodes were placed on the same face of an unidirectional CFRP coupon of 500x260 mm and 3 mm thickness.

One of the electrodes covered the entire width (260 mm) of the coupon whereas the second was a small square electrode (50x50) centered at the half of the width (mid electrode).

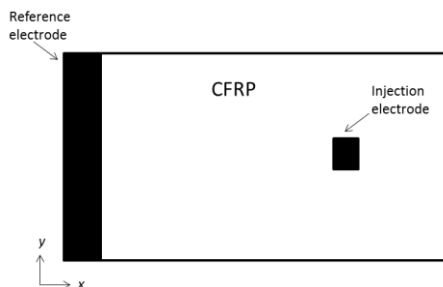


Fig. 1. Geometry of the CFRP coupon and the electrodes. This view corresponds to the electrode side. The other side was not equipped with electrodes. Reference axes x (axes of the carbon fibers) and y are indicated.

The electrodes and the CFRP coupon were submitted to compression force by means of mechanical C-clamps.

B. Experiment procedure

Both faces of the CFRP were ink marked forming an array of equidistant points. A DC power supply was connected to both electrodes being the reference electrode connected to the common (ground). Potential at all marked points including the side without electrodes have measured. Since the measured points were symmetrical, the computation of the potential differences between both faces of the coupon can be obtained.

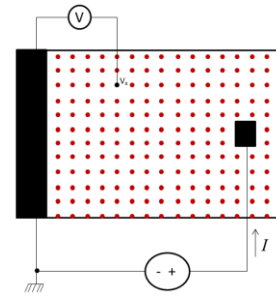


Fig. 2. Experiment setup. Red dots are the points where potential V_x is measured. A symmetrical array of marks is available on the other face (side without electrodes).

C. Results and discussion

Although the injected current reached several amperes, the results have been normalized to 1 A. Fig. 3 shows the experimental results. Fig. 3a plots the potentials at the electrode face whereas Fig. 3b plots the potentials at the opposite face. The differences of potentials between both faces are depicted in Fig. 3c.

The potentials below the mid electrode presented in Fig. 3a should be in the form of equipotential lines parallel to the mid electrode down to the reference electrode (see Fig. 4). However the resulted potentials were more irregular. These irregularities would correspond to some deficiencies in the contact between the electrodes and the CFRP. Although pressure was applied to the CFRP and electrodes, the electric contacts still were not uniform.

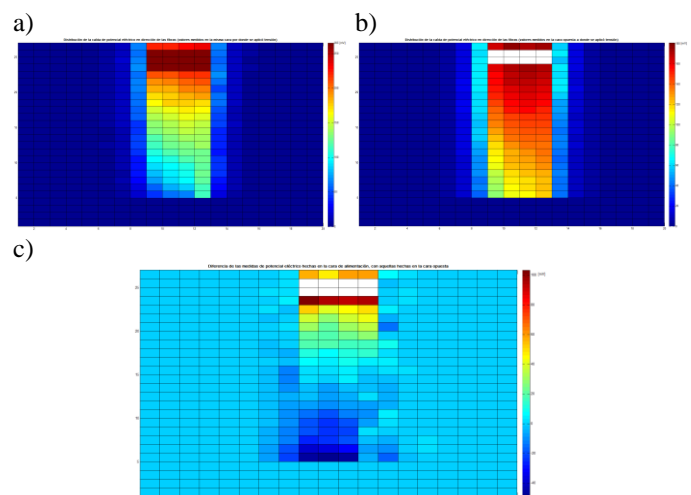


Fig. 3 a) Potential measured at the electrodes side. b) Potential measured at the opposite side. c) Potential differences between both sides. White squares correspond to points that were not possible to obtain the potential due to obstacles.

Potentials on both coupon faces were not equal. The face where electrodes were placed presented higher potentials and more asymmetry along the vertical axes of the electrodes.

That is assumed to be due to contact defects. On the other side, potentials were about 5/7 lower than the ones in the electrode face but presented more symmetry. The electrodes face presented higher potential gradients along the electrodes axes compared to the opposite face. The difference of potentials between both faces shows two peaks. One peak was located at the edge of the mid electrode and the second peak at the edge of the reference electrode. Both peaks had different polarity due to the differences in potential gradients on both surfaces. The sign reversal was produced about half of the distance between electrodes.

In order to study the asymmetry of potential in the electrodes face, the experiment was modelled by means of the Finite Element Method. The CFRP coupon was modelled with an anisotropic electrical conductive body. The electrodes were considered to be perfect conductors and with a perfect contact with the CFRP.

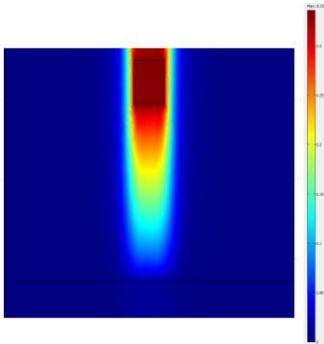


Fig. 4 FEM simulation of the potential distribution

The simulation results are presented in Fig. 4. The obtained potential distribution agrees with the experimental but presents symmetry along the vertical axis of the electrodes. As suggested before, the lack of symmetry in the real coupon may be due to deficiencies in the electrical contacts. These results suggest a practical method for the verification of CFRP connections on full scale wind turbine spars. The method is described in the next section D.

D. Minimal invasive method for evaluate the effectiveness of the CFRP connections in real spars

The method is illustrated by means of a simplified CFRP spar geometry with two electrodes at each end (Fig. 5). These electrodes correspond to the lightning protection system (LPS) bonding of the wind turbine spar. The CFRP spar is allowed to conduct lightning currents and is part of the LPS [4].

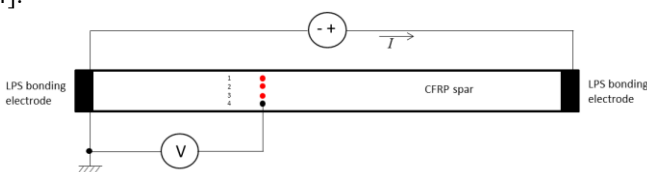


Fig. 5 CFRP spar with two LPS bonding electrodes at each end. A DC power supply, the required voltmeter and illustrative measurement locations (red dots) are provided.

After manufacturing a CFRP spar, it is difficult to determine defects of connections of the LPS bonding electrodes. In wind turbine blades, these electrodes may be composed of a cables, plates, meshes, foils or some depositions, but here we treat them as a single electrodes. If the electrodes are not able to produce a uniform contact, due to the anisotropic properties of CFRP, the current will not be uniformly distributed. This may pose a serious danger since very high lightning current densities can produce delamination.

The method proposed here is based on the potential measurements conducted on the CFRP coupon. But now the entire spar is considered. The procedure can be performed after the manufacturing of the spar (or the blade depending on the manufacturing process). As before, a DC current shall be injected, so almost one of the electrodes must be disconnected from the LPS. Then, in a selected radius the voltages from a reference electrode will be measured perpendicular to the spar axis (e.g. red marks 1 to 4 of Fig. 5). From the obtained values, the differences between voltages $V_j = V_k + \Delta v_k$ would indicate different current densities along the paths. If no difference between V_j and V_k is found, we can assume that the paths of the currents along the measured points will have the same current density. But if some difference is present ($\Delta v_k \neq 0$), then the current densities may be different. If $\Delta v_k < 0$ it means that less current will flow along the path between electrodes passing through k compared to the path passing j . The method also allows to study transitions in the geometry of the CFRP and it is suggested to be applied at several radius.

III. THERMAL IMAGING OF DC AND IMPULSES

Another method to infer the current density distribution through the CFRP coupon is done by measuring thermal effects (e.g. see application in[8] and references therein). Joule heating could show current paths up on the coupon surface. Several tests are presented, the first with same configuration and the rest with different electrodes setup. For each test, voltage and current were measured in order to compute electric charge ($\int i dt$) and integral action ($\int i^2 dt$).

A. Case I

First, the same setup as employed in section II was tested (Fig. 7).

a)

**Preprint of the:
Asia-Pacific International Conference on Lightning (APL),
2015
Nagoya, Japan**

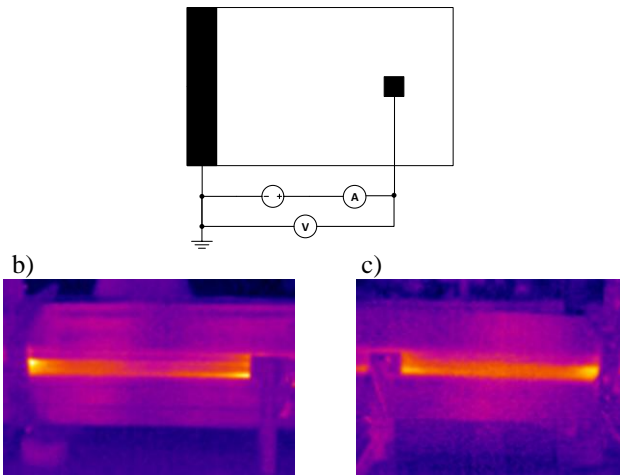


Fig. 7 a) Test configuration. b) Thermal image from the electrodes side. c) Thermal image from back side.

Thermal images show how the temperature is higher along the path (x direction) between the mid electrode and the reference. The temperature rise is mostly confined to the mid electrode width suggesting a low diffusion of the current in the other directions. That is due to the high conductivity on the x direction.

B. Case II

Now the mid electrode was moved to the opposite side (Fig. 8). In this case, thermal images show lower temperatures which correlate with lower current through the coupon. Due to the electrodes are in different sides of the coupon and z -conductivity is lower than x -conductivity, the current is much lower compared to Case I. Both sides show the same behavior and the width of the highest temperature path fits with the mid electrode width as before.

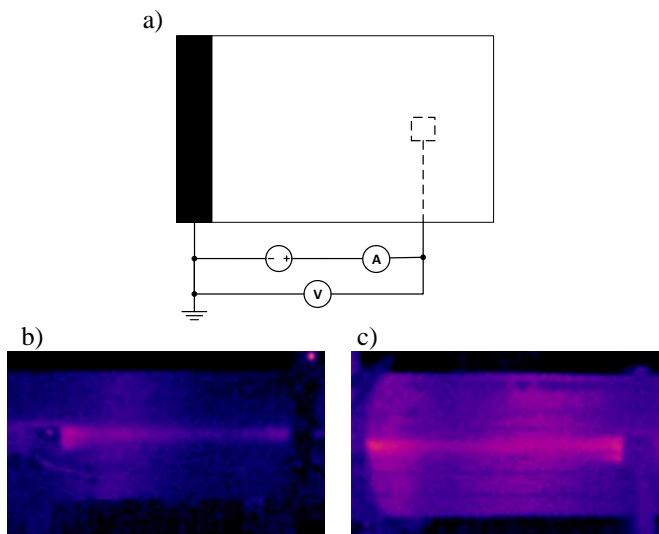


Fig. 8 a) Test configuration. b) Thermal image from the reference electrode side. c) Thermal image from the mid electrode side.

C. Case III

Next, two small electrodes were connected in the same side but they were faced one each other as indicates Fig. 9a.

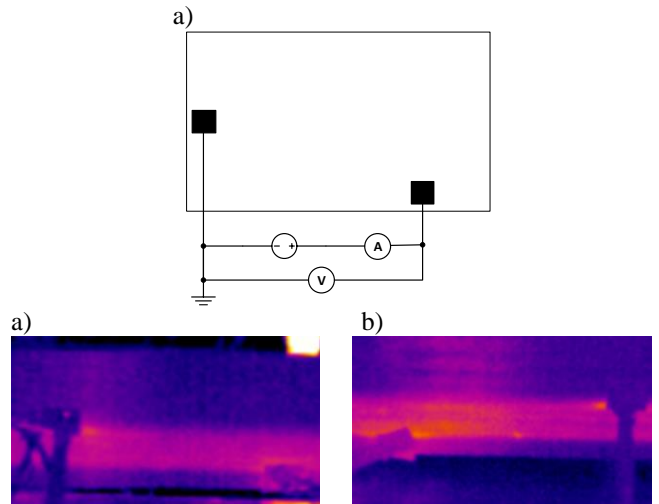


Fig. 9 a) Test configuration. b) Thermal image from the electrodes side. c) Thermal image from the opposite side.

Although the electrodes were located at the same side those were not faced each other. The displacement in the y direction produced a temperature rise along the x direction in the area corresponding to the y displacement.

D. Case IV

The next has the setup indicated in Fig. 10a. In this arrangement, two small electrodes were faced each other but displace along the y direction.

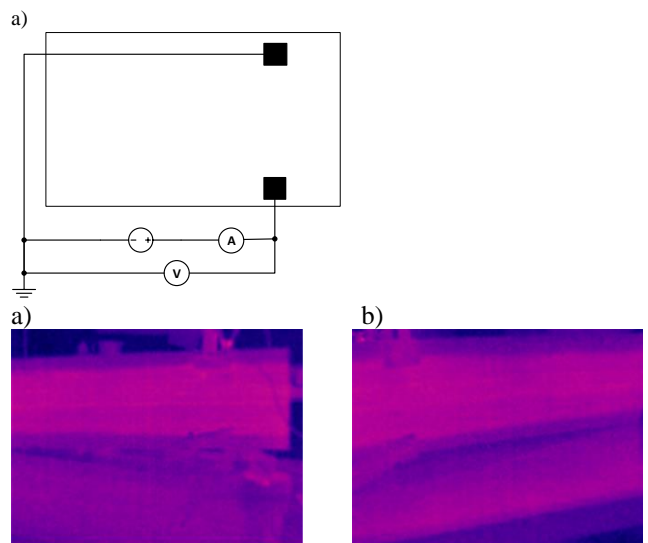


Fig. 10 a) Test configuration. b) Thermal image from connections side. c) Thermal image from opposite side.

Preprint of the:
Asia-Pacific International Conference on Lightning (APL),
2015
Nagoya, Japan

In this case it is interesting to realize that although the electrodes are separated in the y direction the temperature increase appears all along the coupon in area with a width corresponding to the distance between the electrodes.

E. Case V

The last experiment (Fig. 11) presented in this paper corresponds to a similar geometry of Fig. 7a but with a larger mid electrode. In this case a 8/20 μ s current impulse of 23 kA was applied.

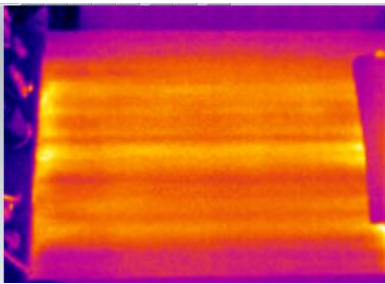


Fig. 11 Thermal image of the electrode side.

Although the applied charge was lower than the DC cases, the integral action was three orders of magnitude higher. The temperature distribution clearly suggests that the current was not uniformly distributed probably due to some irregularities of the connections. After removing the electrodes some small damages were found indicating electric arcs.

IV. CONCLUSIONS

In this paper we obtained the surface potentials for DC currents in a CFRP coupon. Potentials of both faces have been measured and the potential difference between symmetrical points of both faces has been computed. A new method for full scale CFRP spars has been proposed. By means of thermal imaging the distribution of DC and impulses currents have been investigated. The results presented here provide new information useful for lightning protection of CFRP in wind turbine spars and CFRP components used in aircrafts.

ACKNOWLEDGMENT

This study was supported by research grants from the Spanish Ministry of Economy and Competitiveness

(MINECO)AYA2011-29936-C05-04,ESP2013-48032-C5-3-R, and Centre for the Development of Industrial Technology (CDTI) EEA GRANTS project IDI-20140071. The authors wish to thank LABLEC high voltage laboratory to allow test execution.

REFERENCES

- [1] J. Montanyà, O. van der Velde, and E. R. Williams, "Lightning discharges produced by wind turbines," *J. Geophys. Res. Atmos.*, vol. 119, pp. 1455–1462, 2014.
- [2] F. Rachidi, M. Rubinstein, J. Montanyà, J. L. Bermudez, R. Rodriguez, G. Solà, and N. Korovkin, "Review of current issues in lightning protection of new generation wind turbine blades," *IEEE Trans. Ind. Electron.*, vol. 55(6), pp. 2489–2496, 2008.
- [3] S. Yokoyama et al., "Lightning Protection of Wind Turbine Blades", *Electra*, pp. 42-45, June 2014.
- [4] Wind turbines - Part 24: Lightning protection, IEC standard, 2010.
- [5] D. Romero, J. Montanyà and J. Vink, "Test and simulation of lightning current distribution on a wind turbine blade," in *Proc. of the 32nd Intl. Conf. on Lightning Protection (ICLP)*, Shanghai, China, October 2014.
- [6] A. Piche, I. Revel, and G. Peres, "Experimental and Numerical Methods to Characterize Electrical Behaviour of Carbon Fiber Composites Used in Aeronautic Industry," *Advances in Composite Materials - Analysis of Natural and Man-Made Materials*, Dr. Pavla Tesinova (Ed.), InTech, 2011.
- [7] R. Abid, A. Haddad, H. Griffiths, D. Clark, M. Coleans and S. Evans, "Electrical Characterization of Aerospace Graded Carbon Fiber Reinforced Plastic Composites Under Low Current DC and Impulse Energizations," in *Proc. of the Intl. Conf. on Lightning and Static Electricity*, Seattle, SU, September 2013.
- [8] T. Nishi, H. Tsubata, and H. Fujita, "Lightning Current Flow Analysis and Measurement of the Composite Structure," in *Proc. of the Intl. Conf. on Lightning and Static Electricity*, Seattle, SU, September 2013.